Performance Evaluation of Full-Scale Sections of Asphalt Pavements in the State of Qatar

Husam Sadek, S.M.ASCE[1]; Eyad Masad, F.ASCE[2]; Okan Sirin, Aff.M.ASCE[3]; Hussain Al-Khalid[4]; and Khaled Hassan[5]

Abstract: The population and economy in the State of Qatar have been increasing in the past 5 years. Accordingly, traffic loading has also increased rapidly, which affected the performance of existing roads and highways. This high traffic loading merits consideration of the design and construction of long-lasting pavements that require minimal maintenance. The Transport Research Laboratory (TRL) in collaboration with the Public Works Authority (PWA) of Qatar constructed a field experiment that consisted of six different pavement sections in order to investigate the influence of using different materials and asphalt mixture designs on performance. This paper presents a comprehensive study for the field evaluation of the performance of these trial sections. The evaluation involved the use of the falling weight deflectometer (FWD) and a vehicle equipped with instruments for measuring permanent deformation and cracking. These field measurements were complemented with laboratory measurements on field cores: the dynamic modulus, flow number, and semicircular bending tests. The results revealed that the increase in temperature between winter and summer in Qatar reduced the stiffness of asphalt mixtures by about 80%. The sections in which polymer-modified bitumen was used had the lowest temperature susceptibility. Moreover, the results showed that the bitumen and aggregate type significantly affected the stiffness and the trial sections' resistance to rutting and fracture. **DOI: 10.1061/(ASCE)CF.1943-5509.0000627.** © *2014 American Society of Civil Engineers.*

Author keywords: Falling weight deflectometer (FWD); Dynamic modulus; Perpetual pavement; Mechanistic-empirical pavement design; Semicircular bending; Qatar.

Introduction

The construction of highways and road networks in many countries in the Middle East region has experienced remarkable development both in size and standards in the last 40 years. However, only a few regional research studies have been conducted to evaluate and improve the performance of asphalt pavements. Several of these studies focused on studying the effect of significant increase in traffic loading and hot weather on rutting (Al-Abdul Wahhab et al. 1994, 2001). Bubshait (2001) asserted that the main reason for pavement failures in the region is that materials are not carefully selected and mixtures are not designed to suit regional conditions. For example, unmodified 60–70 Pen bitumen is used widely in the Middle East; however, this bitumen is too soft given the high temperatures in the region. Fatani et al. (1992), Al-Abdul Wahhab et al. (1994), and Elseifi et al. (2012) suggested the use of either a harder bitumen or a polymer-modified bitumen (PMB) to mitigate poor performance that is associated with the use of unmodified 60–70 Pen bitumen.

In the State of Qatar, there have been significant efforts in the past 5 years on developing better specifications for pavement materials. These efforts were motivated by the rapid increase of traffic loading, and the realization that current specifications do not accommodate the international developments in material tests and improvement of properties. The high traffic loading merits consideration of the design and construction of *long life* or perpetual pavements. Many studies in the United States, Europe, and the Far East showed the significantly improved performance of perpetual pavements in terms of resistance to surface distresses and deteriorations when compared to conventional or *determinate life* pavements (Ferne 2006; Merrill et al. 2006; Timm and Newcomb 2006). The concept of perpetual pavement design implies prevention of the onset of deterioration in the form of rutting and fatigue cracking in the structural layers, which is a result of increased traffic loading and high temperatures. The design of perpetual pavements could be achieved by reducing the stress and strain in the pavement either by increasing the thickness of the pavement layers and/or by using specific materials for each layer that assists in resisting the potential distresses in these layers (Merrill et al. 2006; Renteria and Hunt 2008).

The review of literature revealed that only a few field studies have been conducted in the countries within the Arabian Peninsula to evaluate the benefits of using mechanistic-empirical design and the construction of perpetual pavements (Al-Abdul Wahhab et al. 1994, 2001; Masad et al. 2011; Sadek et al. 2014). Most of these studies focused on characterization of local materials, influence of significant increase in traffic loading on performance, and rutting due to high temperature. This paper reports on the findings from a

[1]Ph.D. Student, Centre for Engineering Sustainability, School of Engineering, Univ. of Liverpool, Brodie Tower, Brownlow St., Liverpool L69 3GQ, U.K. (corresponding author). E-mail: hsadek@liverpool.ac.uk

[2]Professor, Mechanical Engineering Program, Texas A&M Univ. at Qatar, 253 Texas A&M Engineering Building, Education City, P.O. Box 23874, Doha, Qatar. E-mail: eyad.masad@qatar.tamu.edu

[3]Assistant Professor, Dept. of Civil and Architectural Engineering, College of Engineering, Qatar Univ., P.O. Box 2713, Doha, Qatar. E-mail: okansirin@qu.edu.qa

[4]Centre for Engineering Sustainability, School of Engineering, Univ. of Liverpool, Brodie Tower, Brownlow St., Liverpool L69 3GQ, U.K. E-mail: H.Al-Khalid@liverpool.ac.uk

[5]Regional Manager-Middle East, Transport Research Laboratory (TRL), Qatar Foundation, Qatar Science and Technology Park, P.O. Box 210529, Doha, Qatar. E-mail: khassan@trl.co.uk

Note. This manuscript was submitted on June 9, 2013; approved on May 7, 2014; published online on September 8, 2014. Discussion period open until February 8, 2015; separate discussions must be submitted for individual papers. This paper is part of the ***Journal of Performance of Constructed Facilities***, © ASCE, ISSN 0887-3828/04014123(14)/$25.00.

comprehensive study that was conducted to investigate the effect of material properties and mixture design on performance of asphalt pavements.

Scope and Objectives of the Study

The Public Works Authority (PWA) of the State of Qatar has developed several programs and initiated projects to enhance the specifications and design of pavements. One of these programs is the "Road Pavement Technology" project with the Transport Research Laboratory (TRL), which involved reviewing pavement design and performance besides developing new pavement designs for the State of Qatar. For this purpose, a field experiment was performed to investigate the influence of materials and mixture design on performance. This experiment involved the construction of six different pavement sections in Qatar. The sections were constructed in 2010 on a route used by heavy truck traffic. The conditions, performance, and mechanical properties of these sections were monitored after 3 years of service by conducting the following tests and measurements:

- Falling weight deflectometer (FWD) tests during the spring and summer seasons in order to evaluate the stiffnesses of pavement layers;
- Automatic road analyzer vehicle in order to measure pavement rutting;
- Dynamic modulus ($|E^*|$) test on field cores to assess the stiffness of asphalt mixtures;
- Flow number (FN) test on field cores to assess the resistance to rutting; and
- Semicircular bending (SCB) test in order to evaluate the fracture resistance of the mixtures.

In addition to the preceding tests, mechanistic-empirical analysis was performed to evaluate the performance of these pavement sections after 3 years and also after 20 years.

Description of Field Trial Sections

Six different asphalt pavement sections, about 150 m lengths each, were constructed in 2010 as a part of an access road to a sand processing plant in the south of Qatar. The location shown in Fig. 1 was selected due to its high traffic loading on the trial sections.

Fig. 2 shows all trial sections were designed and constructed to have thick asphalt layers. As discussed before, the sections were designed in order to evaluate the influence of type of bitumen, type of aggregate, and type of mixture design on performance.

Fig. 3 illustrates the layers and materials used in each section. The aggregate used in the surface course for all trial sections was Gabbro imported from United Arab Emirates. This is an igneous rock that has been used in road construction and concrete structures for long time in this region. The difference among the surface course layers is in the mixture design and bitumen type. The asphalt base course used in these sections differed in bitumen type, aggregate type, and mixtures design. The same granular subbase with limestone aggregate was used for all sections. The estimated design modulus for the subbase is 450 MPa (TRL Report C 2010; TRL Report D 2010). The subgrade is weathered limestone with a design modulus of 200 MPa (TRL Report C 2010; TRL Report D 2010; Sadek et al. 2012).

Section 4 is the control section that was designed based on the standards of Qatar Construction Specifications (QCS), which is essentially the Marshall method. The percentage refusal density (PRD) design method [BS EN 12697/32:2003 (2003); TRL 2002] was used in all other sections. The PRD test is used to determine the

Fig. 1. Location of trial sections in Qatar (image © 2014 Google; map data © 2014 Google)

design asphalt content at which the refusal density is 3% in the voids in mineral aggregate (VMA). This requirement is supposed to ensure that deformation will not occur to reduce percentage air voids to lower than 3% in the field. This design method includes other criteria to achieve durable mixture and field compaction.

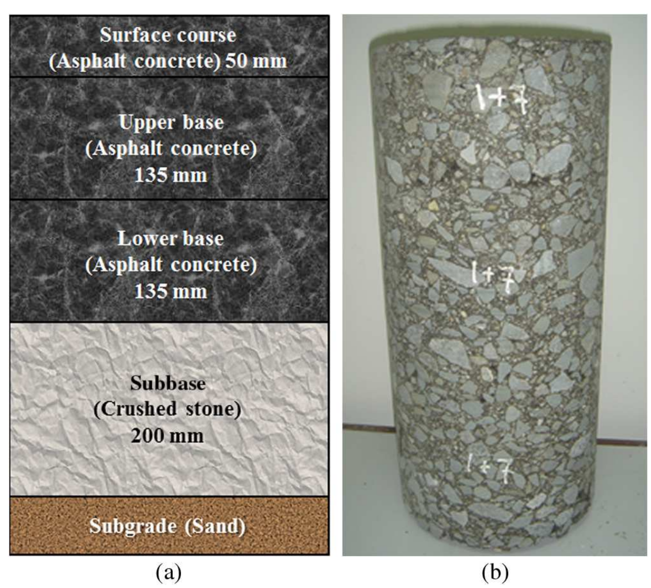

Fig. 2. (a) Typical cross section of trial sections; (b) core extracted from the trial site

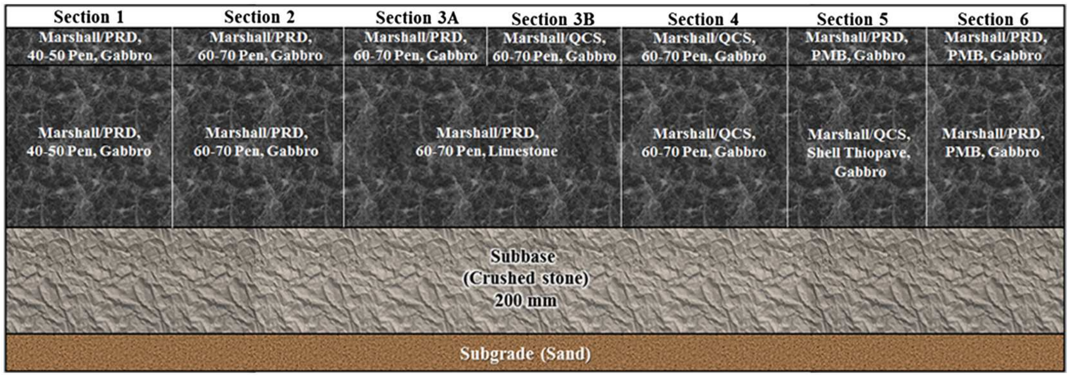

Fig. 3. Layers and materials' properties of all trial sections

Section 5 included the use of Shell Thiopave, which is a sulphur extended asphalt, while Section 6 included PMB with an SBS modifier. Pen 60–70 base bitumen was used in developing the modified asphalts. Limestone, which is a local aggregate in Qatar, was used in the base course in Section 3 to compare it with the performance of sections in which Gabbro was used. One day after paving, three pairs of cores were taken from each trial section and tested for compositional analysis as shown in Table 1.

Since the opening of the trial road in August 2010, about 1,800 trucks pass daily in each direction; about 50% of the trucks are fully loaded with sand (45 t). Based on the traffic data, three axle configurations of trucks are passing the trial road 6 days a week: five-axle; four-axle; and three-axle trucks. The total axle load equivalent factors for these trucks were calculated to be 11.33, 10.5, and 4.5, respectively. These values are considered to be very high, which led to the high 20-year ESALs of 115.4 million. Table 2 summarizes the traffic loading calculation. Up to the point when the field measurements were performed in summer 2013, traffic has reached approximately 17 million ESALs.

Field Testing and Results

In order to monitor the performance of the trial sections, several field and laboratory tests were conducted on these sections. The field work started in January 2012 with collecting pavement condition data by the automatic road analyzer vehicle as shown in Fig. 4(a). This vehicle is instrumented to measure rutting. The FWD test, shown in Fig. 4(b), was also conducted to evaluate pavement structural condition by acquiring the deflections of each layer. These deflections were used to back-calculate the moduli of the various layers [asphalt concrete (AC), granular subbase, and subgrade] using Elmod6 software (Dynatest Elmod6 version 6.1.44). The FWD test was conducted in February (spring season) and August (summer season) in 2012 to monitor the temperature susceptibility of the trial sections at low and high temperatures.

Fig. 5 shows ten cores with each core having a diameter of 150 mm and a height of 320 mm that were extracted from each trial section.

For laboratory testing, a total of 12 field cores, 2 replicate samples from each section, were tested to determine the $|E^*|$ and the FN [AASHTO designation: TP 79-11 (AASHTO 2011)] using the asphalt mixture performance tester (AMPT) as shown in Fig. 6(a). Another six cores, one from each section, were subjected to the monotonic SCB test using the facility at the University of Liverpool in United Kingdom to assess the fracture resistance of each section as shown in Fig. 6(b).

FWD Test Results

The FWD test was conducted twice on the trial road. The first test was conducted in the spring season (February 2012), the average air temperature was about 23°C while the average surface temperature was about 25°C. The second test was conducted in the

Table 1. Compositional Analysis Summary for All Trial Sections

Section	Mix design	Bitumen content (%)	Stability (kN)	Flow (mm)	Stiffness (kN/mm^2)	VIM (%)	VMA (%)	VFB (%)	Filler/bitumen ratio
	Surface course								
1	PRD	3.9	14.8	2.6	6.2	4.0	14.2	71.7	1.49
2	PRD	3.8	14.7	2.6	5.7	4.9	14.3	69.1	1.35
3A									
3B	QCS	3.8	13.4	2.7	5.2	5.3	14.8	64.4	1.11
4									
5	PRD	3.8	14.4	2.5	5.8	4.7	14.1	68.5	1.42
6									
	Base course								
1	PRD	3.6	15.2	3.1	4.9	4.1	13.3	69.0	1.75
2	PRD	3.4	14.1	2.6	5.5	4.5	13.2	65.8	1.71
3A	PRD	4.4	11.5	2.9	4.0	4.2	14.2	71.2	1.23
3B									
4	QCS	3.5	14.1	2.6	5.4	4.8	13.7	64.9	1.31
5	QCS	3.9	NA	NA	NA	NA	NA	NA	1.13
6	PRD	3.5	15.2	2.6	5.9	4.2	13.2	67.9	1.48

Table 2. Traffic Loading Calculation

Axle configuration	Trucks/day (both lanes)	Trucks/year	Fully loaded truck factor	One year ESALs (million)	20-year ESALs (million)
Five-axle	600	0.19×10^6	11.33	2.2	44
Four-axle	1,000	0.31×10^6	10.5	3.3	66
Three-axle	200	0.06×10^6	4.5	0.27	5.4
Total	1,800	0.56×10^6	—	5.77	115.4

summer season (August 2012); the average air temperature was 46°C while the average surface temperature was about 63°C. Fig. 7 shows the moduli values for the various layers back-calculated using Elmod6.

As would be expected, the results illustrate that the moduli of the AC layer and subbase layer are higher at the lower temperature. The difference in moduli between the two seasons was the highest for the asphalt layer because of the temperature dependency of the asphalt behavior. The difference between the moduli of the two seasons for the subgrade results was relatively small.

In general, it can be stated that the AC layer, with PMB, in Sections 5 and 6 had the lowest temperature susceptibility, while Section 2, with 60–70 Pen bitumen, had the highest temperature susceptibility. This result showed that modified bitumen reduced the temperature's impact on the stiffness of the asphalt pavement layers.

The moduli for the AC layers of the various sections in the summer time were very close to each other (≈2,000 MPa) in contrast to the spring season. Fig. 7 shows that the stiffness of the asphalt mixtures decreased by around 80% between the spring and summer seasons.

Analysis of variance (ANOVA) was conducted to test the statistical differences among the moduli for each of the layers. The analysis was done using statistical significance level of 5% (using $\alpha = 5\%$). In this analysis, the p-value is the probability of acquiring a test statistic at least as extreme as the one that was actually observed, assuming that the null hypothesis is true. One often *rejects the null hypothesis* when the p-value is less than the predetermined significance level α indicating that the observed result would be highly unlikely under the null hypothesis. Table 3 shows the summary and results of ANOVA.

Based on the results in Table 3, the p-value of the HMA layer is less than 0.05. So, the null hypothesis is rejected and 95% confident that the mean modulus of this layer is not statistically equal among the trial sections. For the subbase and subgrade layers, the p-value is more than 0.05 and this means that 95% confident that the mean modulus for each of the layers is not statistically significant among the trial sections.

Rutting Results from Automatic Road Analyzer Vehicle

The wire model algorithm was employed for measuring rut depth using the automatic road analyzer vehicle. The wire model

(a) (b)

Fig. 4. (a) Automatic road analyser vehicle collecting data from site; (b) FWD test conducted on the site

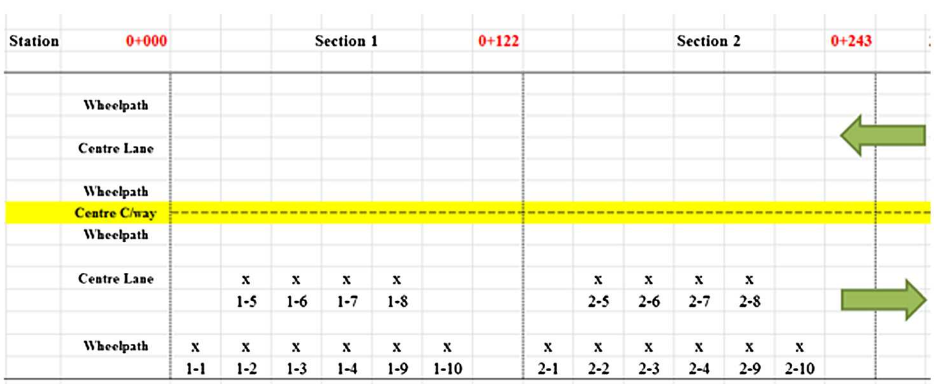

Fig. 5. Location and layout of cores

Fig. 6. (a) AMPT for dynamic modulus and flow number tests; (b) set up for monotonic SCB test

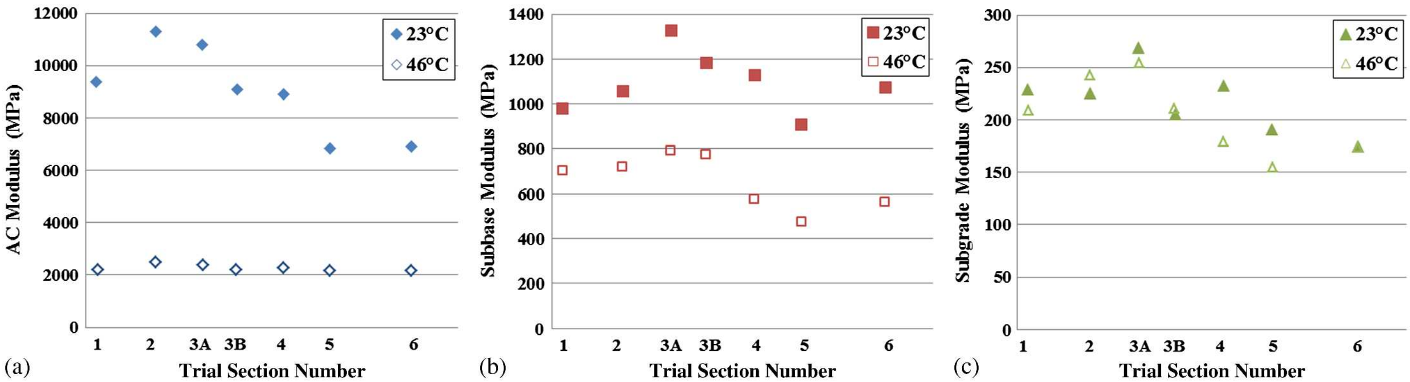

Fig. 7. Comparison between moduli of each layer in low and high air temperatures

Table 3. ANOVA Summary and Results for Dynamic Modulus Results of Each Layer

Section	Count	Sum	Average	Variance	*p*-value
			HMA layer		
1	10	93,686	9,368	5,672,269	6.71×10^{-8}
2	8	90,309	11,288	6,263,932	
3A	6	64,705	10,784	5,821,235	
3B	8	72,691	9,086	3,529,195	
4	8	71,147	8,893	4,488,666	
5	25	170,850	6,834	2,210,381	
6	13	90,004	6,923	1,103,870	
			Subbase layer		
1	10	9,795	979	102,693	0.079
2	8	8,458	1,057	147,928	
3A	6	7,954	1,325	295,126	
3B	8	9,461	1,182	64,248	
4	8	9,032	1,129	1,11,667	
5	25	22,736	909	68,243	
6	13	13,945	1,072	67,584	
			Subgrade layer		
1	10	2,289	228	5,234	0.082
2	8	1,803	225	9,335	
3A	6	1,611	268	12,541	
3B	8	1,642	205	529	
4	8	1,856	232	7,132	
5	25	4,762	190	3,380	
6	13	2,266	174	2,186	

algorithm within the vehicle system connects the high points on the pavements transverse profile and establishes the rut depth under these points as shown in Fig. 8. The vehicle has 1,028 data points across the 4-m transverse profile; the data was filtered down to 40 data points across that profile. From that the wire model will connect the high points across a 3-m stretch centered along the profile; the model will then take the highest distance from the wire to the pavement for either 1.5-m side or record that has the left/right wheel path rut depth.

The values of rut depth were taken as an average of 10 values (1 value/m). Fig. 9 shows an example of rutting data collected by the automatic road analyzer vehicle for trial Section 1. Table 4 shows the average of maximum rut depth for both directions was obtained to compare the trial sections against rutting. In general, it was observed that all sections of the road had little rutting.

The effect of using different bitumen but same aggregate and mix design was one of the major targets of this study. Thus, trial Sections 1, 2, and 6 were compared. Table 4 shows that Section 2 has the highest rutting depth value. This section consists of a surface course and a base of percentage refusal density design (PRD) with 60–70 Pen bitumen and the aggregate used was Gabbro. This concludes that Section 6 with PMB bitumen performed slightly better than Sections 1 and 2.

Then, a comparison between pavement Sections 2 and 3A was conducted to assess the influence of using the local aggregate, limestone, in resisting rutting. Both sections consist of a surface course and a base of PRD design with 60–70 Pen bitumen but with different

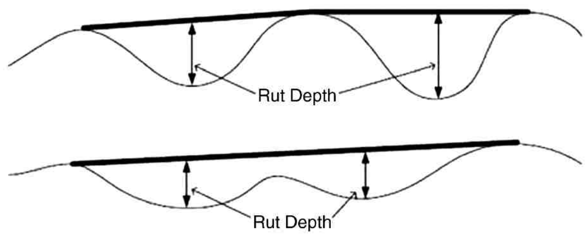

Fig. 8. Rut depth measurement using the wire model algorithm

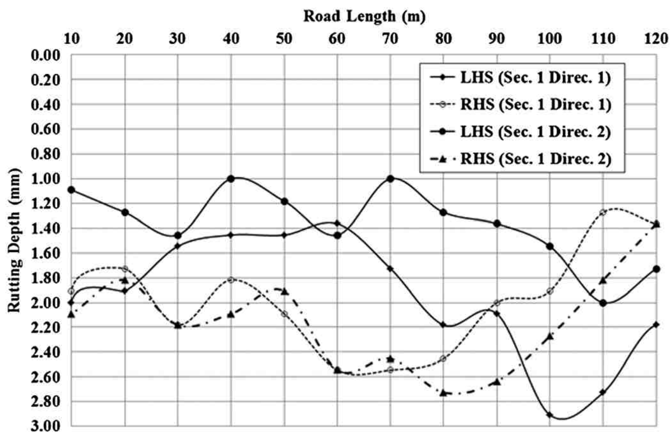

Fig. 9. Rutting depth values measured by the road analyzer vehicle for trial Section 1

aggregate type for the base. From the results shown in Table 4, it can be concluded that the difference between both sections in rut depth was negligible.

In addition, a comparison between trial Sections 2 and 4 with Gabbro aggregate and between 3A and 3B with limestone were conducted to assess the effect of mix design. It is shown that trial Section 2 has higher rut depth value than Section 4. On the other hand, the rut depth is marginally higher for Section 3B than Section 3A. The results show that the mix design didn't affect significantly the rut depth results.

Finally, rut depth values for trial Sections 5 and 6 were compared to evaluate the effect of having different base layer. Both sections consist of a surface course of PRD with PMB bitumen but different base layer. From the table, it was shown that Section 5 has a higher rut depth value than Section 6. These results showed that using Shell Thiopave in the base did not affect the performance of the pavement section significantly.

In general, it was observed in the field that the full-scale trial road had little rutting. However, all trial sections performed very similar against rutting after 2 years of service.

Table 4. Rut Depth Results for All Trial Sections

Section	Average of maximum rut depth for both lanes (mm)
1	2.73
2	3.06
3A	2.97
3B	3.10
4	2.55
5	2.97
6	2.53

Laboratory Testing and Results

The dynamic modulus ($|E^*|$), flow number (FN), and SCB tests were used for evaluating the asphalt mixtures in terms of rutting susceptibility, fatigue, and fracture resistance in laboratory and field performance. The $|E^*|$ and FN are key tests within the simple performance test (SPT) suite. They were developed under NCHRP Project 9-19 and applied in the Superpave mix design procedure (Witczak et al. 2002; Bonaquist et al. 2003; Zhu et al. 2011). Recently, Mohammad et al. (2011) conducted FN, dynamic modulus, and SCB tests on HMA mixtures containing high-reclaimed asphalt pavement (RAP) content with crumb rubber additives. The results showed that the aforementioned tests are useful to characterize the mixtures and discriminate between them.

The SCB test, first proposed by Chong and Kuruppu (1984), has been widely used by researchers to evaluate the fracture resistance of asphalt mixtures by loading several specimens with different notch depths monotonically until failure. Molenaar et al. (2002), Elseifi et al. (2012), and Kim et al. (2012) described this test as a rapid and simple test to be performed on easy to prepare specimens. These advantages made this test preferable than other tests such as bending beam test and favored by many researchers. From the results of this test, the maximum tensile stress, resilient modulus, fracture toughness (or stress intensity factor, K), and fracture energy of HMA mixtures can be determined (Molenaar et al. 2002; Ozer et al. 2009; Othman 2011). In a study by Arabani and Ferdowsi (2009), the ability of the SCB test to characterize the tensile strength and fracture toughness of mixtures was compared to a set of common static and dynamic tests. The results showed the SCB test to be reliable and having good correlation with fracture parameters obtained from other fracture tests.

Dynamic Modulus Test Results

The $|E^*|$ test is a nondestructive test that is used to measure the dynamic modulus and phase angle for each trial section. A total of 12 specimens collected from the base layer of each section were cored and prepared to standard size of 100 mm diameter and 150 mm in height. A repeated load, with zero confinement, was applied at 4.4, 21.1, 37.8, and 54°C with loading frequencies of 25, 10, 5, 1, 0.5, and 0.1 Hz [AASHTO designation: TP 79-11 (AASHTO 2011)]. In this study, 21.1°C was taken as the reference temperature. Master curves were developed from the test data using a sigmoidal fitting function proposed by Pellinen et al. (2002). The sigmoidal function can be described as follows:

$$\mathrm{Log}(|E^*|) = \quad \delta + \frac{\alpha}{1 + e^{\beta+\gamma(\log \xi)}} \tag{1}$$

where δ = minimum modulus value; α, β, and γ = regression coefficients for the fitting function; and ξ = reduced frequency. Table 5 and Fig. 10 shows the master curves and shift parameters.

Generally, the dynamic modulus values for all mixtures are significantly high compared to results reported in other studies in literature (Goh et al. 2011; Kim et al. 2009; Zhu et al. 2011; Bonaquist 2010). The range of $|E^*|$ values are similar to the values from a previous study by Masad et al. (2011) conducted on field cores prepared using modified PG 76-22 bitumen and extracted from a major freeway in Qatar. Fig. 10 shows that, at the high reduced time and temperature end, Sections 6 and 3B exhibit highest $|E^*|$ values, which implies these two sections are the most resistant to rutting. The range of $|E^*|$ values is an indication that mixture designs used in Qatar can be too stiff, which raises a concern about the durability and fatigue resistance of these mixtures.

Table 5. Master Curve and Shift Parameters

Section	δ	α	β	γ	A	b	c
1	2.867	3.864	−1.634	0.490	0.0009	−0.166	3.062
2	2.708	3.933	−1.807	0.438	0.001	−0.168	3.086
3B	3.168	3.266	−1.663	0.414	0.0009	−0.164	3.028
4	0.109	6.581	−2.324	0.363	0.0011	−0.177	3.208
5	3.613	3.006	−1.594	0.552	0.0008	−0.157	2.939
6	3.277	3.319	−1.534	0.422	0.0009	−0.164	3.044

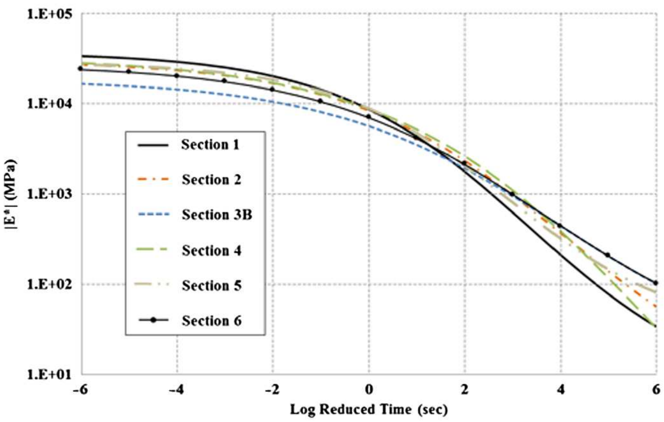

Fig. 10. Dynamic modulus master curves for all trial sections

In order to study the effect of using different bitumen types on mixture stiffness, master curves of trial Sections 1, 2, and 6 and then Sections 4 and 5 were compared as shown in Figs. 11(a and b), respectively. Both figures show that all compared sections had high dynamic modulus values at low reduced time (high frequency) and temperature. In contrast, the stiffness of Section 1, with 40–50 Pen bitumen, in Fig. 11(a) became lower than the other Sections 2 and 6 at high-reduced time and temperature. This inferred that modified bitumen make AC layers stiffer at high temperature than those of unmodified bitumen, which improves the permanent deformation resistance. In addition, PMB flattened the master curve of Section 6 and reduced the effect of temperature and frequency on the stiffness.

Fig. 11(b) showed no difference at low reduced time (high frequency) and temperature between using 60–70 Pen and Thiopave bitumen when the mix design is QCS and the aggregate used is Gabbro. The difference is considerable at high-reduced time and temperature where Section 5 with Thiopave is stiffer than Section 4 with 60–70 Pen bitumen.

After that, $|E^*|$ master curves of Section 2, with Gabbro, and Section 3B, with limestone, were compared to assess the effect of using different aggregate types as shown in Fig. 11(c). Section 3B had higher dynamic modulus than that of Section 2 at high-reduced times and temperatures. This result demonstrated that using the local aggregate (limestone) increased the stiffness of the mixture in this study, which is affecting positively on its performance against rutting.

In Fig. 11(d), a comparison between master curves of Sections 2 (Marshall/PRD) and 4 (Marshall/QCS) is shown. The effect of using different mix designs was evaluated here. Both sections performed the same at low-to-intermediate reduced times while Section 2 has a slightly higher dynamic modulus value at very high reduced time or temperature. It can be stated that Marshall/PRD and Marshall/QCS design mixes did not have much effect on the stiffness of both sections.

From all preceding comparisons, it was noticed that the type of bitumen and aggregate mainly affected the dynamic modulus of HMA mixes in the trial sections.

FN Test Results

The specimens were subjected to FN test using the AMPT following the methods described in NCHRP 465 and 513 reports. The FN test, which is also called as repeated load test in some studies, was performed at a temperature of 54.4°C with zero confinement under 137 kPa deviatoric stress up to 10,000 cycles or until achieving 50,000 cumulative permanent microstrain. In this test, the higher the FN value, the better is the trial section resistance to permanent deformation. Fig. 12 illustrates the FN test results for the six HMA mixtures considered in this study.

All FN values are high when compared to those published in several previous studies conducted in the United States under similar conditions (Mohammad et al. 2006; Wang et al. 2011; Apeagyei et al. 2011; Kanitpong et al. 2012). This high FN value is an indication that these mixtures are expected to have high resistance to rutting. This is a result of the mixture designs used which utilize fully crushed aggregate, relatively low bitumen content when compared with mixtures in the United States, and are developed based on specifications that emphasize the high resistance to permanent deformation given the high temperature expected in Qatar and the region.

To assess the sensitivity of using different bitumen on the resistance of mixtures against rutting, FN results of Sections 1, 2, and 6 and then Sections 4 and 5 were compared. Fig. 12 presented that Section 1, with 40–50 Pen bitumen, and Section 2, with 60–70 Pen bitumen, had very close FN values while Section 6, with PMB, had slightly lower FN value. On the other hand, Fig. 12 shows that Section 5 with Thiopave bitumen had a lower FN value than the control Section 4 and this could be attributed to aging characterization or the volumetric of the mix. In general, all of them performed well against rutting but the results proved that the bitumen type and grade are important factors in rut resistance of HMA mixes. The FN was found to increase with increasing the bitumen grade while the use of modified bitumen did not improve the performance of the mixture (Bonaquist 2010).

Then, FN results of Section 2, with Gabbro, and Section 3B, with limestone, were compared to evaluate the influence of using different aggregate types. Section 2 had significantly higher FN cycles than that of Section 3B. This result demonstrated that using the local aggregate (limestone) decreased the ability of the mixtures to resist rutting. This can be attributed to the relatively low angularity of limestone, which is one of the main factors affecting the reduction of the FN value and shows low rut resistance.

Also, the effect of using different mix designs was assessed by comparing FN results of Sections 2 (Marshall/PRD) and 4 (Marshall/QCS). Both sections performed the same and showed similar resistance against rutting. This observation confirms that the mix design is not a main factor in rut resistance of HMA mixes.

Conferring to the preceding comparisons, it was clearly observed that the type of the bitumen and aggregate angularity mainly affects resistance of permanent deformation for asphalt mixtures.

Monotonic SCB Test Results

The configuration of the SCB test consists of three-point monotonically increasing compressive loading that induces tension in the bottom part of a SCB specimen. The set up of the test consists of two supporting rollers at the bottom edge and a loading roller at the midpoint of the semicircular arch (Liu 2011; Mull et al. 2002).

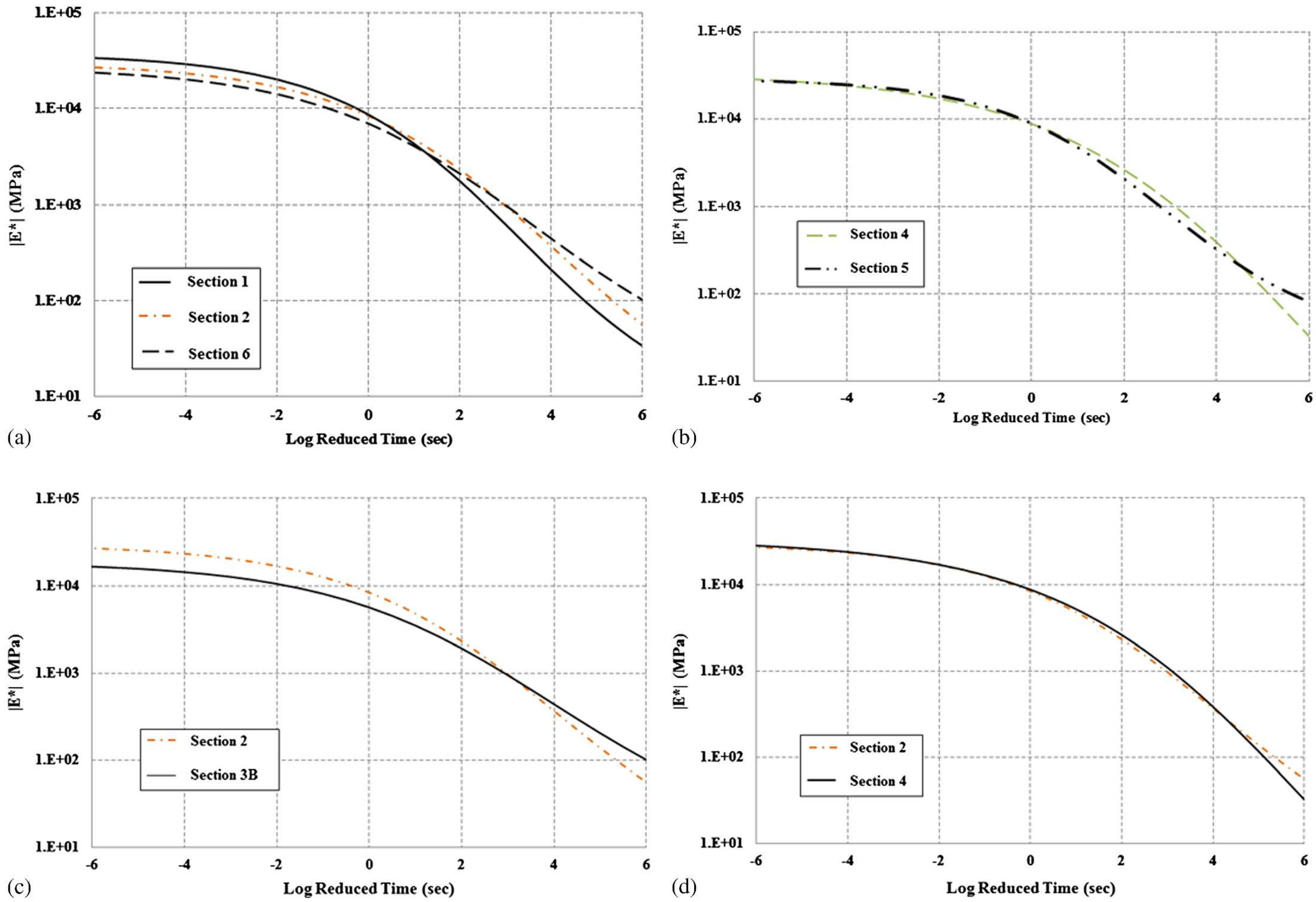

Fig. 11. Dynamic modulus master curves for (a) Sections 1, 2, and 6; (b) Sections 4 and 5; (c) Sections 2 and 3B; (d) Sections 2 and 4

The spacing between the two supports is 0.8 times the diameter as shown in Fig. 13(a).

For the purpose of evaluating the fracture resistance of the trial sections, one core from each section was tested in the laboratory of the University of Liverpool. These six cores consisted of a surface course (≈70 mm) and a base course (≈250 mm). The base course of each core was cut symmetrically from the middle of the specimen into two circular slices, each 50 mm in height. Fig. 13(b) shows each slice was symmetrically cut into two semicircular samples with a notch of 12.5 mm (0.5 in.).

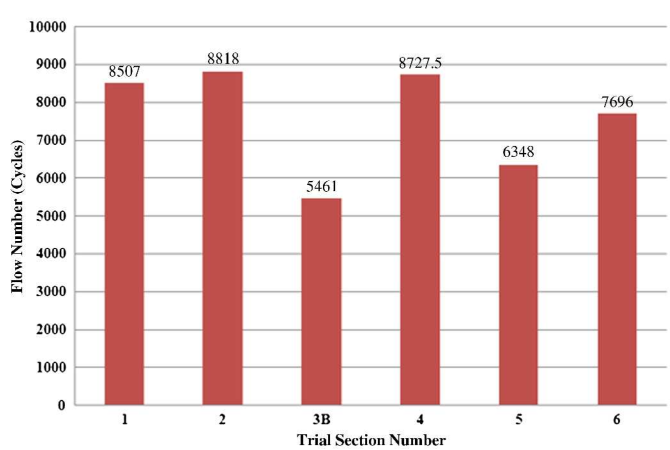

Fig. 12. Flow number test results for each trial section

Two semicircular specimens from each core were then subjected to the monotonic SCB test and the applied load was strain-controlled at 5 mm/min and at temperature of 10°C. The other half of semicircular specimens was tested at 10 mm/min at the same temperature to investigate the effect of loading rate on the performance of the mixtures. The applied load, the horizontal and vertical displacement in addition to the measured stress and strain were monitored and recorded during the test. This test data was used to calculate the fracture toughness, fracture energy, and maximum tensile stress at the bottom of specimens of each section using the equations shown in Table 6.

Fig. 14 illustrates the stress-strain curve for each trial section obtained from the tests at 5 mm/min. It was observed from the test that materials were brittle and failed abruptly with little deformation or plastic flow. Also, Fig. 14 shows no well-defined peaks or slow fracture tail, common with softer materials and slower test speeds. Fig. 15 illustrates the summary of the results of both SCB tests for each trial section in this study.

Generally, the fracture toughness, fracture energy and maximum tensile stress values of all mixtures are high and reflected good performance when compared with published values for other mixtures. However, Section 1, Marshall/PRD with 40–50 Pen bitumen and Gabbro, had the highest average fracture parameters among the trial sections. This high resistance to propagation to fracture is primarily caused by the stiffness of these mixtures.

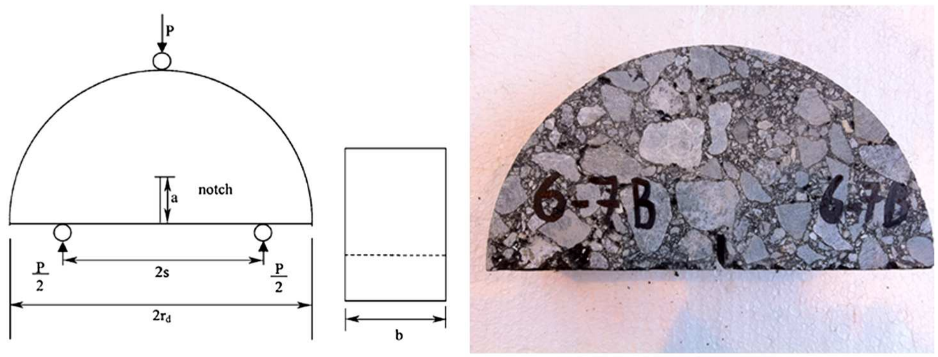

(a) (b)

Fig. 13. (a) Typical set up for SCB test; (b) notched SCB test specimen

It is documented that mixtures with high stiffness have good resistance to fatigue cracking and fracture when they are used in thick sections, while they have low resistance to fatigue when used in thin pavement sections (Masad et al. 2008; Tayebali et al. 1994). These mixtures are all used in thick sections in this experiment so they are expected to have very good resistance to bottom-up fatigue cracking because the stress at the bottom of the layer would be very small. However, given their high stiffness, these mixtures would be expected to have problems with fatigue cracking if used in thin sections or if the bond between the surface course and base course is compromised. In addition, the very high stiffness of mixtures with low asphalt content might contribute to problems in durability and top-down cracking.

To evaluate the significance of bitumen on the resistance to fracture, Sections 1, 2, and 6 were compared. Fracture toughness and fracture energy of field samples are affected by bitumen type as concluded by Li et al. (2006). In Fig. 15(a), the sections were compared based on the fracture toughness. The results showed that Section 1 with unmodified 40–50 Pen bitumen had the highest fracture toughness in both loading rates. This is the case for fracture energy and maximum tensile stress.

After that, Sections 4 and 5 with QCS mix design and Gabbro were compared to evaluate the significance of using Shell Thiopave bitumen on the resistance of fracture. In Figs. 15(a and c), the results showed that both sections had very similar fracture toughness and maximum tensile stress values at both loading rates. However, the case for fracture energy is different as shown in Fig. 15(b). Section 5, with Thiopave bitumen, dissipated more energy to propagate the crack than Section 4 with unmodified 60–70 Pen bitumen. Generally, it can be stated that Thiopave bitumen improved the performance of the mixture in fracture resistance.

The performance of Sections 2 and 3B were assessed to acquire insight into the effect of aggregate type by comparing their results of fracture toughness, fracture energy, and tensile stress as shown in Fig. 15 as well. The results of Section 3B in the test of lower loading rate (5 mm/min) were ignored because the specimen was highly segregated. Generally, the result demonstrated that both sections had very fracture resistance but Section 2, with Gabbro, outperformed with higher fracture energy than Section 3B, with limestone, as shown in Fig. 15(b).

Then, the influence of mix design on the fracture resistance was evaluated by comparing the use of Marshall/PRD in Section 2 and Marshall/QCS in the control Section 4. From results shown in Fig. 15, it can be stated that using the conventional mix design Marshall/QCS had a little bit more toughness, energy, and tensile stress than PRD mix design. The small difference between both results emphasized that mix design is not a main factor affecting the fracture resistance compared to bitumen or aggregate type.

Table 6. Equations Used to Calculate Fracture Toughness, Fracture Energy, and Tensile Stress

Parameter	Equation used	Reference
Fracture toughness (K)	$K = \left(\frac{P}{2rt}\right) Y_1 \sqrt{\pi a}$	Lim et al. (1993)
Fracture energy (G_f)	$G_f = \frac{W}{A_{Lig}}$	RILEM TC 50-FMC (1985)
Maximum tensile stress at the bottom of the specimen (σ)	$\sigma = 3.564 \frac{P_{ult}}{D.t}$	Shu et al. (2010)

Note: ΔP = applied load (N); a = notch depth (mm); A_{Lig} = ligament area (mm^2); D = specimen diameter (mm); P_{ult} = ultimate applied load (N); r = specimen radius (mm); t = specimen thickness (mm); W = work of fracture (kN · mm); Y_1 = normalized stress intensity factor in mode I.

Mechanistic-Empirical Analysis for Performance Evaluation

The researchers at Texas A&M University at Qatar developed a pavement analysis tool for the analysis of asphalt pavement performance. This analysis tool uses the same fatigue and rutting models in the Mechanistic-Empirical Pavement Design Guide (M-E PDG) software, and it is programmed in Excel.

Fig. 16 shows the inputs of the developed pavement analysis tool were the structure and properties of the pavement layers; the dynamic modulus values obtained from $|E^*|$ laboratory tests,

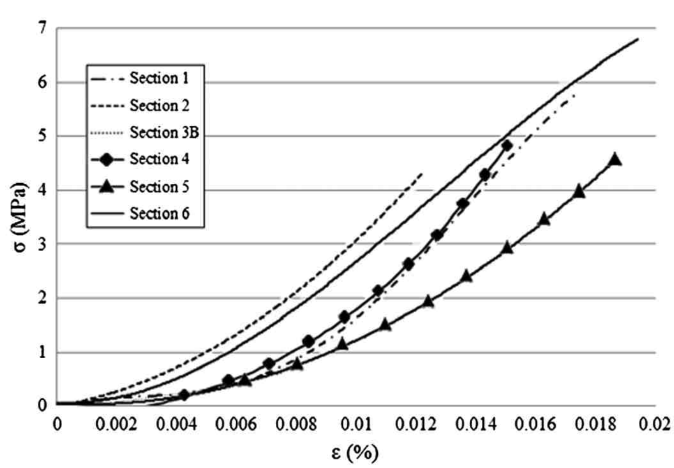

Fig. 14. Stress-strain curves obtained from SCB test for all mixtures at 5 mm/min

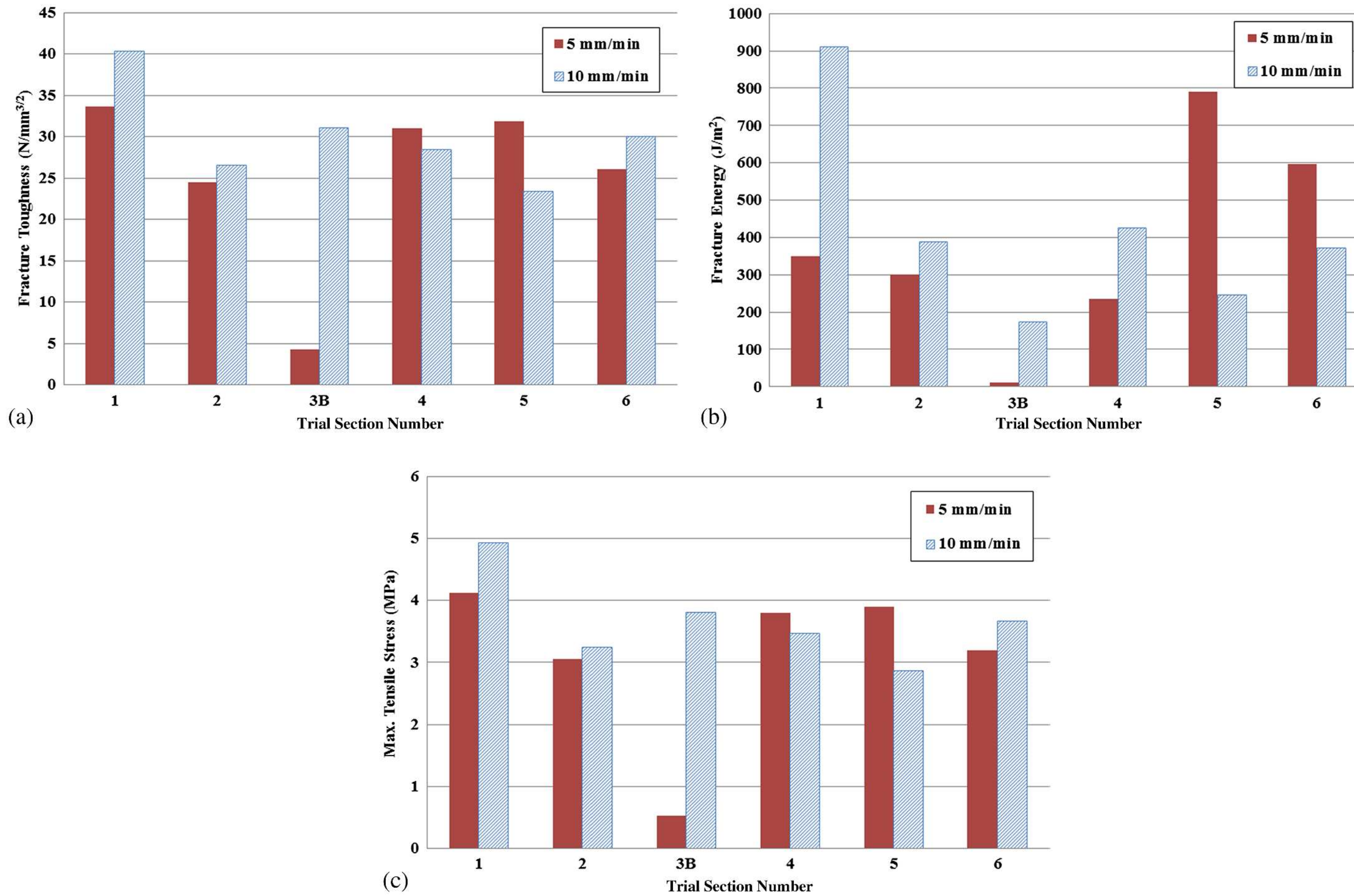

Fig. 15. Comparison between all trial sections for both loading rate: (a) fracture toughness; (b) fracture energy; (c) maximum tensile stress

the air temperature, the responses of the pavement layers of the trial sections from a linear elastic software (WinJULEA) obtained from FWD results, and finally the traffic loading data after 3 years of service. Then, it predicts the fatigue damage in terms of alligator (bottom-up) cracking and it can also measure the expected rutting depth in each layer and in every season separately.

In order to predict the alligator cracking and rutting depth, the following models from *M-E PDG* software were used:

$$\text{Fatigue (Alligator) Cracking} = \frac{100}{1 + e^{c_2'(-2+\log FD)}} \tag{2}$$

where FD = the fatigue damage that is calculated from actual number of traffic loads within a specific time divided by the number of allowable repetitions to failure for bottom-up cracking (N_f); where N_f = determined using the tensile strain at the bottom of AC thick layer acquired from WinJULEA analysis with its dynamic modulus $|E^*|$ value obtained from the laboratory test; c_2' = a calibration factor, which depends on the thickness of the AC layer and is calculated as follows:

$$c_2' = -2.40874 - 39.748\ (1 + h_{AC})^{-2.856} \tag{3}$$

Then, permanent deformation (rutting depth) is calculated as follows:

$$\text{Permanent Deformation (Rutting)} = \sum_{1}^{m} h_i \varepsilon_{p(AC)_i} \tag{4}$$

where h_i = thickness of AC sublayer i; and $\varepsilon_{p(AC)i}$ = vertical plastic strain of AC sublayer i which is calculated by Eq. (5).

$$\varepsilon_{p(AC)_i} = \varepsilon_{v(AC)_i}(\beta_1 k_1 10^{-\beta_2 3.35412} T^{\beta_3 1.5606} N^{\beta_4 0.4491}) \tag{5}$$

where $\varepsilon_{v(AC)i}$ = vertical compressive strain at middepth of AC sublayer i obtained from WinJULEA analysis; $\beta_{1,2,3,4}$ = regional

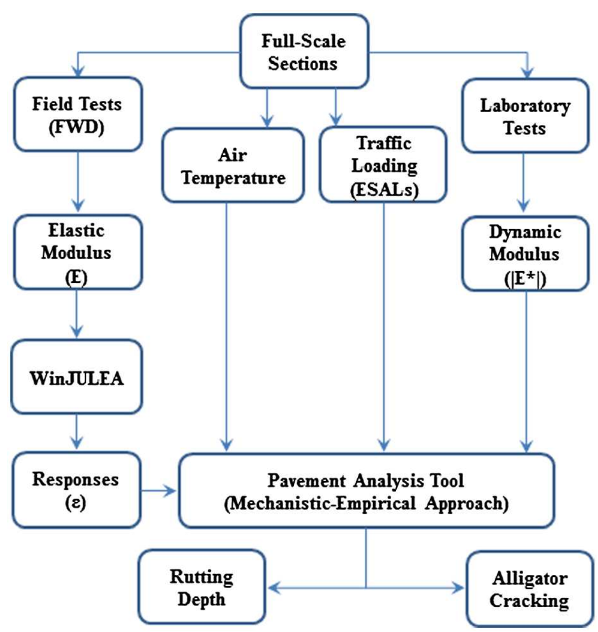

Fig. 16. Developed pavement analysis tool flow chart

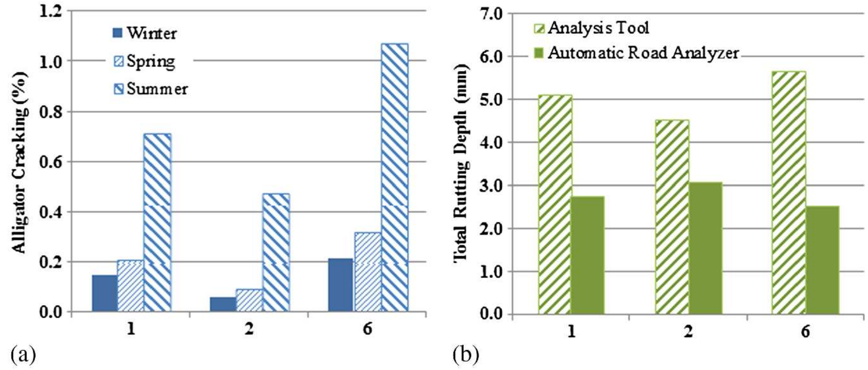

Fig. 17. Pavement analysis tool results for trial Sections 1, 2, and 6: (a) alligator cracking; (b) rutting depth

calibration factors which are assumed to be 0.7 based on preliminary work conducted by researchers in Texas A&M at Qatar; k_1 = coefficient calculated from the thickness of the AC layer; T = pavement surface temperature that is calculated from the recorded air temperatures for three seasons in Qatar using SHRP models available in Mohseni et al. (2005); and N = actual number of traffic loads (ESALs).

The performance models implemented in this tool were used to conduct comparative analysis of the performance of the different pavement sections. These models need to be calibrated in the future based on comprehensive field measurements.

Effect of Bitumen

The trial Sections 1, 2, and 6 were compared to check the influence of bitumen type on the performance of the mixes against alligator cracking and rutting in different seasons. The results of alligator cracking in Fig. 17(a) for these three trial sections were significantly low and this is complying with the field observations. This was expected because of the use of perpetual pavement concept in the trial sections (Sadek et al. 2014). In Fig. 17(b), the comparison indicated that total rutting depths obtained from the automatic road analyzer vehicle is lower than those calculated using the analysis tool for traffic loading of 2 years only. The rutting model in the analysis tool needs to be further calibrated to better match field results in the future. In general, the type/grade of bitumen did not affect the performance significantly after 2 years of loading. Generally, the performance of Section 2, with 60–70 Pen bitumen, had the lowest cracking percentage and rutting depth.

Then, Sections 4 and 5 were also compared to evaluate the impact of bitumen type on the performance of the mixes against fatigue and rutting in different seasons when the QCS mix design was used. As the previous comparison, the results of alligator cracking in Fig. 18(a) for these two sections were significantly low as observed in the field. In general, the results showed that using Shell Thiopave bitumen didn't affect the alligator cracking percentage a lot compared to unmodified bitumen especially when the temperature is high. In Fig. 18(b), again, the comparison specified that total rutting depths attained from the road analyzer vehicle is greatly lower than those calculated using the analysis tool for traffic loading of 2 years only. From the figures, the total alligator cracking and the total rutting depth are higher for Section 5 with Thiopave than those for trial Section 4.

Effect of Aggregate Type

Comparing Sections 2 and 3B assessed the impact of using limestone as an alternative of Gabbro. The performance of the trial sections against fatigue cracking (alligator) and rutting in different seasons was evaluated. Fig. 19(a) showed that Section 2, with Gabbro, and Section 3B, with limestone, had very low cracking percentage (less than 0.5%). The results of the road analyzer and the pavement analysis tool were not matching; however, it showed that there was no significant difference in the rutting resistance if limestone was used as alternative of Gabbro as shown in Fig. 19(b).

Effect of Mix Design

The effect of using altered mix designs was studied by comparing the performance of Sections 2 and 4 in resisting alligator cracking in addition to rutting. Fig. 20(a) concluded that the alligator cracking values for both sections are very small and negligible but

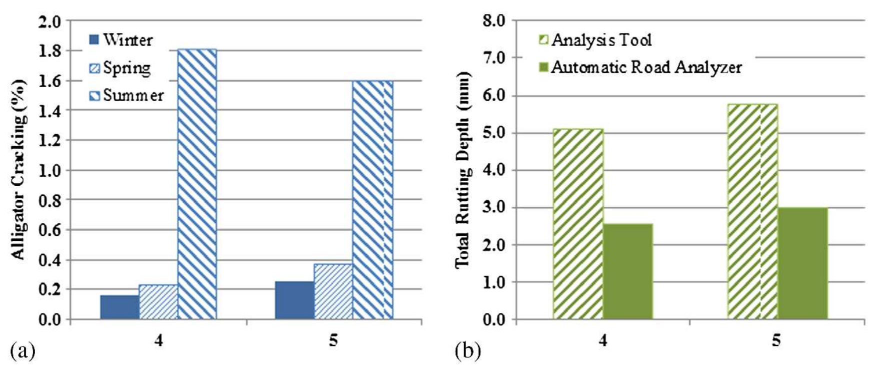

Fig. 18. Pavement analysis tool results for trial Sections 4 and 5: (a) alligator cracking; (b) rutting depth

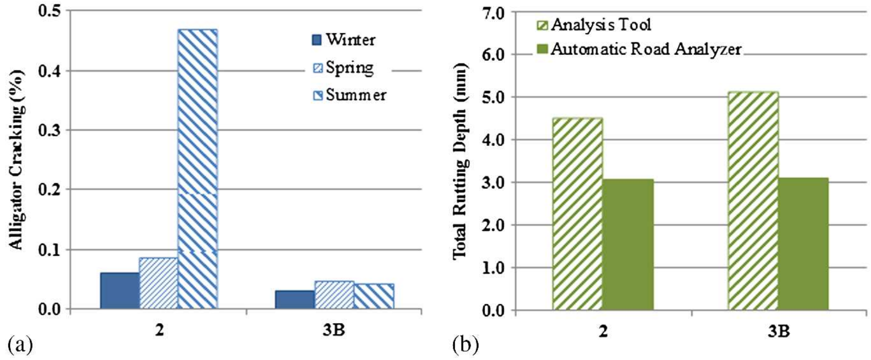

Fig. 19. Pavement analysis tool results for trial Sections 2 and 3B: (a) alligator cracking; (b) rutting depth

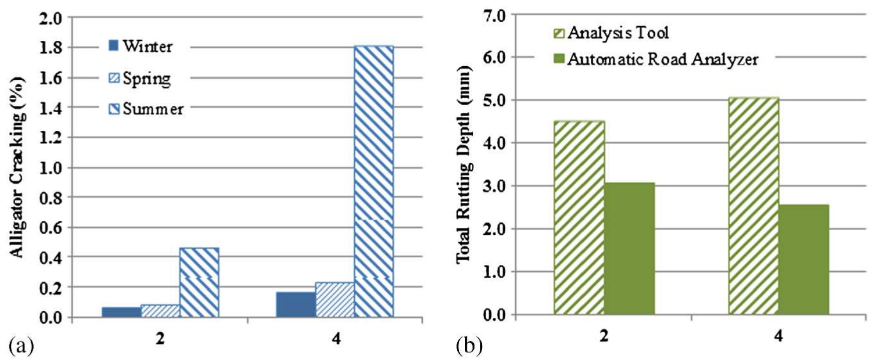

Fig. 20. Pavement analysis tool results for trial Sections 2 and 4: (a) alligator cracking; (b) rutting depth

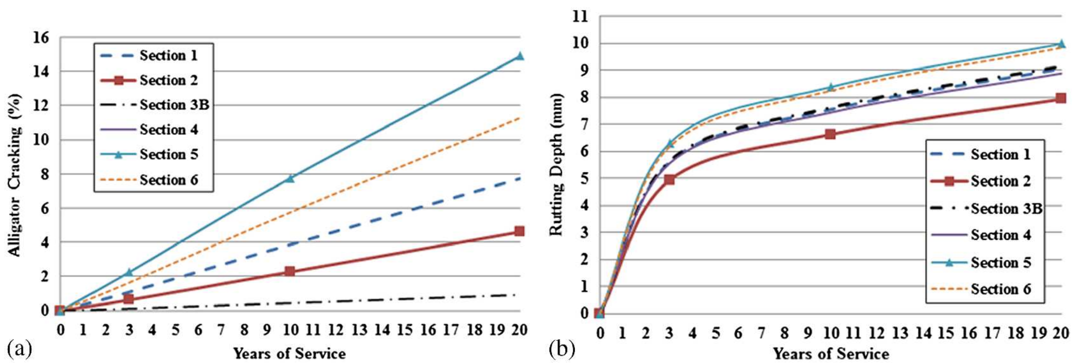

Fig. 21. Pavement analysis tool predicted results for 20 years: (a) alligator cracking; (b) rutting depth

Section 2, PRD mix design, showed better resistance than QCS mix design in Section 4. Similar to the previous subsections, Fig. 20(b) showed that the rutting results of the road analyzer did not match with the results of the analysis tool but there was no significant difference in performance between PRD and QCS mix designs.

In addition, Fig. 21 shows that the developed pavement analysis tool can be used to predict the performance after 10 or 20 years.

According to all preceding comparisons, the results of alligator cracking are complying with field observations and thus could be predicted by the developed pavement analysis tool while rutting model needs further calibration to match the field results. Accordingly and based on the fact that Qatar has different conditions than the United States, the value of the first regional calibration factor, β_1, was reduced to be 0.3 and Fig. 22 shows that this can give closer results to the field results.

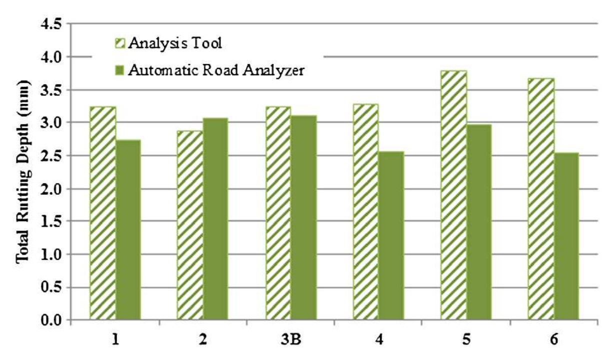

Fig. 22. Rutting depth of all trial sections after reducing β_1

Conclusions

With the aim of assessing the long-term performance of the trial sections, some field and laboratory tests were conducted. The following are the major conclusions based on the results of this study:

- Field and laboratory tests indicated that all trial sections continue to perform very well 3 years after construction;
- According to the results of all tests, only the bitumen and aggregate type significantly affected the stiffness and the trial sections' resistance to rutting and fracture;
- All mixes were generally very stiff and had low rutting depths but Section 6, with PMB bitumen and Gabbro, was the stiffest under condition of high temperature. In contrast, Section 1, with 40–50 Pen bitumen and Gabbro in the base layer, was the least stiff;
- Increase in temperature in Qatar reduced the stiffness of AC layers by about 80%. In addition, at high temperature, all sections had almost the same modulus value of 2,000 MPa measured using FWD;
- Sections 5 and 6, with PMB, had the lowest in temperature susceptibility. However, Section 2, with unmodified 60–70 Pen bitumen, was the highest in temperature susceptibility; and
- The developed pavement analysis tool with mechanistic-empirical functions was very useful to predict the performance of the trial sections against alligator cracking and permanent deformation. The functions will be calibrated against more comprehensive field data.

It is obvious from this study that rutting, fracture, and alligator cracking are not major distresses for the perpetual pavements in Qatar. More laboratory tests will be conducted in the near future to evaluate the fatigue resistance and durability of these sections. Results will help make recommendations for updating the materials and design of asphalt pavements, and determining more of the input parameters for mechanistic-empirical analysis of asphalt pavements in the State of Qatar.

Acknowledgments

The authors would like to acknowledge the financial support provided by Qatar National Research Fund (QNRF) through the National Priority Research Program (NPRP) Project 08-310-2-110. This project was awarded jointly to Texas A&M at Qatar University and Qatar University. The researchers at Texas A&M at Qatar also acknowledge the support through NPRP 4-789-2-293 Project that was used to develop the pavement analysis tool presented in this paper. In addition, the authors would like to extend their gratitude to the Fugro Peninsular Company for its support. Last but by no means least, the authors are indebted to Eng. Mohammed Sadeq for his efforts to develop the pavement analysis tool. The technical input of Dr. Dallas Little during this study is highly appreciated.

References

AASHTO. (2011). "Standard method of test for determining the dynamic modulus and flow number for hot mix asphalt (HMA) using the asphalt mixture performance tester (AMPT)." *TP 79-11*, Washington, DC.

Al-Abdul Wahhab, H. I., Asi, I. M., and Ramadhan, R. H. (2001). "Modeling resilient modulus and temperature correction for Saudi roads." *J. Mater. Civ. Eng.*, 10.1061/(ASCE)0899-1561(2001)13:4(298), 298–305.

Al-Abdul Wahhab, H. I., and Balghunaim, F. A. (1994). "Asphalt pavement temperature related to arid Saudi environment." *J. Mater. Civ. Eng.*, 10.1061/(ASCE)0899-1561(1994)6:1(1), 1–14.

Apeagyei, A. K., Diefenderfer, B. K., and Diefenderfer, S. D. (2011). "Rutting resistance of asphalt concrete mixtures that contain recycled asphalt pavement." *Transportation Research Record 2208*, Transportation Research Board, Washington, DC, 9–16.

Arabani, M., and Ferdowsi, B. (2009). "Evaluating the semi-circular bending test for HMA mixtures." *IJE. Trans. A*, 22(1), 47–58.

Bonaquist, R. (2010). "Wisconsin mixture characterization using the asphalt mixture performance tester (AMPT) on historical aggregate structures." *WHRP 09-03*, Wisconsin Highway Research Program.

Bonaquist, R. F., Christensen, D. W., and Stump, W. (2003). "Simple performance tester for superpave mix design: First-article development and evaluation." *NCHRP Rep. No. 513*, National Cooperative Highway Research Program, Washington, DC.

BS EN 12697/32:2003 (2003). "Bituminous mixtures. Test methods for hot mix asphalt. Laboratory compaction of bituminous mixtures by vibratory compactor." BSI, London, U.K.

Bubshait, A. A. (2001). "Quality of pavement construction in Saudi Arabia." *Pract. Period. Struct. Des. Constr.*, 10.1061/(ASCE)1084-0680(2001)6:3(129), 129–136.

Chong, K. P., and Kuruppu, M. D. (1984). "New specimen for fracture toughness determination for rock and other materials." *Int. J. Fract.*, 26(2), R59–R62.

Dynatest Elmod6 Version 6.1.44. [Computer science]. Dynatest International.

Elseifi, M. A., Mohammad, L. N., Ying, H., and Cooper, S., III (2012). "Modeling and evaluation of the cracking resistance of asphalt mixtures using the semi-circular bending test at intermediate temperatures." *Road Mater. Pavement Des.*, 13(S1), 124–139.

Fatani, M, Al-Abdul Wahhab, H. I., Balgunaim, F. A., Bubshait, A. A., and Al-Dubaiab, I. (1992). "National research project: Evaluation of permanent deformation of asphalt concrete pavement in Saudi Arabia." *Final Rep.*, King Abdulaziz City for Science and Technology, Riyadh, Saudi Arabia.

Ferne, B. (2006). "Long-life pavements—A European study by ELLPAG." *Int. J. Pavement Eng.*, 7(2), 91–100.

Goh, S. W., You, Z., Williams, C., and Li, X. (2011). "Preliminary dynamic modulus criteria of HMA for field rutting of asphalt pavements: Michigan's experience." *J. Transp. Eng.*, 10.1061/(ASCE)TE.1943-5436.0000191, 37–45.

Kanitpong, K., Charoentham, N., and Likitlersuang, S. (2012). "Investigation on the effects of gradation and aggregate type to moisture damage of warm mix asphalt modified with Sasobit." *Int. J. Pavement Eng.*, 13(5), 451–458.

Kim, Y., Lee, H., and Heitzman, M. (2009). "Dynamic modulus and repeated load tests of cold in-place recycling mixtures using foamed asphalt." *J. Mater. Civ. Eng.*, 10.1061/(ASCE)0899-1561(2009)21:6(279), 279–285.

Kim, Y.-R., Zhang, J., and Ban, H. (2012). "Moisture damage characterization of warm-mix asphalt mixtures based on laboratory-field evaluation." *Constr. Build. Mater.*, 31, 204–211.

Li, X., Zofka, A., Li, X., Marasteanu, M., and Clyne, T. R. (2006). "Investigation of the low-temperature fracture properties of three MnROAD asphalt mixtures." *Final Rep., MN/RC-2006-15*, Minnesota Local Road Research Board, St. Paul, MN.

Lim, I. L., Johnson, I. W., and Choi, S. K. (1993). "Stress intensity factors for semi-circular specimens under three-point bending." *Eng. Fract. Mech.*, 44(3), 363–382.

Liu, J. (2011). "Fatigue life evaluation of asphalt rubber mixtures using semi-circular bending test." *Adv. Mater. Res.*, 255–260, 3444–3449.

Masad, E., Castelo Branco, V., Little, D., and Lytton, R. (2008). "A unified method for the analysis of controlled-strain and controlled-stress fatigue testing." *Int. J. Pavement Eng.*, 9(4), 233–246.

Masad, E., Kassem, E., and Little, D. (2011). "Characterization of asphalt pavement materials in the State of Qatar: A case study." *Int. J. Road Mater. Pavement Des.*, 12(4), 739–765.

Mechanistic-Empirical Pavement Design Guide (M-E PDG) Version 6.1.44. [Computer software]. Applied Research Associates—Transportation, Arizona State Univ., Phoenix, AZ.

Merrill, D., Dommelen, A. V., and Gáspár, L. (2006). "A review of practical experience throughout Europe on deterioration in fully-flexible and semi-rigid long-life pavements." *Int. J. Pavement Eng.*, 7(2), 101–109.

Mohammad, L. N., Cooper, S. B., Jr., and Elseifi, M. A. (2011). "Characterization of HMA mixtures containing high reclaimed asphalt pavement content with crumb rubber additives." *J. Mater. Civ. Eng.*, 10.1061/(ASCE)MT.1943-5533.0000359, 1560–1568.

Mohammad, L. N., Wu, Z., Obulareddy, S., Cooper, S., and Abadie, C. (2006). "Permanent deformation analysis of hot-mix asphalt mixtures with simple performance tests and 2002 mechanistic-emperical pavement design software." *Transportation Research Record 1970*, Transportation Research Board, Washington, DC, 133–142.

Mohseni, A., Carpenter, S., and D'Angelo, J. (2005). "Development of SUPERPAVE high-temperature performance grade (PG) based on rutting damage." *J. Assoc. Asphalt Paving Technol.*, 74, 197–254.

Molenaar, A. A. A., Scarpas, A., Liu, X., and Erkens, S. M. J. G. (2002). "Semi-circular bending test: Simple but useful?" *J. Assoc. Asphalt Paving Technol.*, 71, 794–815.

Mull, M. A., Stuart, K., and Yehia, A. (2002). "Fracture resistance characterization of chemically modified crumb rubber asphalt pavement." *J. Mater. Sci.*, 37(3), 557–566.

Othman, A. M. (2011). "Evaluation of hydrated lime effect on the performance of rubber-modified HMA mixtures." *J. Elastomers Plast.*, 43(3), 221–237.

Ozer, H., Aurangzeb, Q., Roberts, G. L., Al-Qadi, I. L., Carpenter, S. H., and Trepanier, J. (2009). "Evaluation of RAP impact on hot-mix asphalt design and performance." *J. Assoc. Asphalt Paving Technol.*, 78, 317–351.

Pellinen, T. K., Witczak, M. W., and Bonaquist, R. F. (2002). "Asphalt mix master curve construction using sigmoidal fitting function with nonliner least squares optimization." *15th ASCE Engineering Mechanics Conf.*, Columbia Univ., New York.

Renteria, R. A., and Hunt, E. (2008). "Super pavements." *Roads Bridges*, 46(6), 47–51.

RILEM Technical Committee 50-FMC. (1985). "Determination of fracture energy of mortar and concrete by means of three-point bend tests on notched beams." *Materials and Structures*, Vol. 106, RILEM Publications SARL, 285–290.

Sadek, H., Masad, E., Sirin, O., Al-Khalid, H., and Little, D. (2012). "The implementation of mechanistic-empirical pavement design method to evaluate asphalt pavement design in Qatar." *5th Eurasphalt & Eurobitume Congress*, EAPA, Brussels, Belgium.

Sadek, H., Masad, E., Sirin, O., Al-Khalid, H., Sadeq, M., and Little, D. (2014). "Implementation of mechanistic-empirical pavement analysis in the State of Qatar." *Int. J. Pavement Eng.*, 15(6), 495–511.

Shu, X., Huang, B., and Vukosavljevic, D. (2010). "Evaluation of cracking resistance of recycled asphalt mixture using semi-circular bending test." *Paving Materials and Pavement Analysis—Proc., 2010 GeoShanghai Int. Conf.*, China, 58–65.

Tayebali, A., Deacon, J. A., Coplantz, J., Harvey, J. T., and Monismith, C. L. (1994). "Mixture and mode-of-loading effects on fatigue response of asphalt-aggregate mixtures." *Asphalt Paving Technology: Proc., Association of Asphalt Paving Technologists Technical Sessions*, Vol. 63, 118–151.

Timm, D. H., and Newcomb, D. E. (2006). "Perpetual pavement design for flexible pavements in the US." *Int. J. Pavement Eng.*, 7(2), 111–119.

TRL. (2002). "A guide to the design of hot mix asphalt in tropical and subtropical countries." *Overseas Road Note 19*, Overseas Centre, Transport Research Laboratory, Crowthorne, Berkshire, U.K.

TRL Report C. (2010). "Phase C: Performance of existing pavement in Qatar." *TRL Client Project Rep. 282*, Transport Research Laboratory, Berkshire, U.K.

TRL Report D. (2010). "Phase D: Design of site trials." *TRL Client Project Rep. 282*, Transport Research Laboratory, Berkshire, U.K.

Wang, H., Al-Qadi, I. L., Faheem, A. F., Bahia, H. U., Yang, S., and Reinke, G. H. (2011). "Effect of mineral filler characteristics on asphalt mastic and mixture rutting potential." *Transportation Research Record 2208*, Transportation Research Board, Washington, DC, 33–39.

WinJULEA. [Computer software]. Engineering Research & Development Center Software.

Witczak, M. W., Kaloush, K., Pellinen, T., El-Basyouny, M., and Von Quintus, H. (2002). "Simple performance test for superpave mix design." *NCHRP Rep. No. 465*, National Cooperative Highway Research Program, Washington, DC.

Zhu, H., Sun, L., Yang, J., Chen, Z., and Gu, W. (2011). "Developing master curves and predicting dynamic modulus of polymer-modified asphalt mixtures." *J. Mater. Civ. Eng.*, 10.1061/(ASCE)MT.1943-5533.0000145, 131–137.